Nonequilibrium structure in sequential assembly

Alexander V. Popov, Galen T. Craven, and Rigoberto Hernandez*
Center for Computational Molecular Science and Technology, School of Chemistry and Biochemistry, Georgia Institute of Technology, Atlanta, Georgia 30332-0400, USA
(Received 4 June 2015; published 9 November 2015)

The assembly of monomeric constituents into molecular superstructures through sequential-arrival processes has been simulated and theoretically characterized. When the energetic interactions allow for complete overlap of the particles, the model is equivalent to that of the sequential absorption of soft particles on a surface. In the present work, we consider more general cases by including arbitrary aggregating geometries and varying prescriptions of the connectivity network. The resulting theory accounts for the evolution and final-state configurations through a system of equations governing structural generation. We find that particle geometries differ significantly from those in equilibrium. In particular, variations of structural rigidity and morphology tune particle energetics and result in significant variation in the nonequilibrium distributions of the assembly in comparison to the corresponding equilibrium case.

DOI: 10.1103/PhysRevE.92.052108 PACS number(s): 05.70.Ln, 82.60.−s, 68.43.Mn, 81.16.Fg

I. INTRODUCTION

Self-organization and assembly of primitive building blocks into superstructures drive the development of novel products that find use in diverse technological and biological applications [1]. Polymerization [2–4], nucleation [5–7], and micellization [8,9] are typical routes by which molecular subunits assemble into a structured state. The control of such processes allows for the development of molecular machinery with desired structural and dynamical properties [10,11]. In the self-assembly of soft materials [12–14], exotic phase behavior, such as quasicrystalline states [15–17] and cluster crystals [18–25], are observed. Thus, the geometries, and corresponding energetic connectivity networks, of the resulting assemblies can be harnessed for use in tailored materials with unique properties.

In equilibrium systems, the assembled geometries can be complex [26–29]; however, the underlying theory is very mature and contingent only on equilibrium thermodynamic arguments. In contrast, the theory for nonequilibrium systems is significantly less advanced [30]. Here, we develop theory for the structure and dynamics of an assembly process in which small motifs are placed sequentially to build larger structures. This insertion mechanism generates assemblies that differ from those generated by systems at thermodynamic equilibrium [31–33], and we describe this process through a set of governing equations with specified rates. The generality of this model allows it to be characteristic of many kinds of arrival phenomena. For example, it can describe adsorption on a substrate [34–36] or in a static framework [37] and therein can be used to optimize the routes for a targeted structure because of the differences between sequential and equilibrium assembly processes.

II. THEORY AND METHODS

In the arrival-initiated assembly process, we consider the sequential insertion of N particles to K initially empty binding sites. When a new particle arrives at the binding sites, there are three possible outcomes: (1) the particle binds to an unoccupied site, (2) the particle binds to an occupied site, or (3) it does not bind to the chosen site and is available for binding to another site in the next step. All these cases may be specified through the binding probability p_n, where n is the occupation number of the site (that is, the number of particles that already occupy the site). If the particle is rejected, the attempt of adding a new particle to the set of binding sites is repeated until it is accepted by a binding site. Any kind of motion of bound particles, position exchange, diffusion, etc., is not allowed. The correlations between different sites are also neglected.

The parameter $\Phi = N/K$ describes the average number of particles in a site. If $N < K$, Φ corresponds to the occupied site fraction (SF) for sites that are at most singly occupied (for which $p_n = 0$ for $n > 0$) arising from the so-called hard sphere interaction. For higher occupancy, the actual occupied SF is defined as $\phi = K'/K$, where K' is the number of occupied sites. We also introduce partial site fractions ϕ_n for the sites occupied by n particles. By construction, $\phi = \phi_1 + \phi_2 + \cdots + \phi_N = 1 - \phi_0$, where ϕ is the probability that a randomly chosen site is occupied by at least one particle.

The probability P_n that a new particle will ultimately be accepted into a site already holding n particles is proportional to the product of the probability ϕ_n that the new particle lands on one of the sites with the occupation number n and the probability p_n that it is accepted by this site, that is,

$$P_n = Q\phi_n p_n, \tag{1}$$

where Q is the constant of proportionality. The coefficient Q is calculated readily from the fact that $\sum P_n = 1$:

$$Q = \left(\sum_{n=0}^{N} \phi_n p_n\right)^{-1}. \tag{2}$$

The "occupation" probabilities P_n from Eq. (1) depend on the ratios p_i/p_j rather than on the "site acceptance" probabilities p_i themselves. Thus, p_i's can be replaced by rates or relative occupation numbers if they are known.

*hernandez@gatech.edu

The average density $\Phi(m) = m/K$ is a function of the number m of added particles and has a maximal value ($= N/K$). Each accepted (added) particle leads to a small increase in Φ by $\Delta\Phi = 1/K$. In the same time, the partial SFs can increase or decrease by the same amount but with different probabilities. Namely, the SF of empty sites ϕ_0 will be decreased by $\Delta\Phi$ with the probability P_0 upon adding one more particle, whereas ϕ_N can only be increased by the same amount with the probability P_{N-1}. Given that m particles have already been added to the system, the master equations for the average SFs read

$$\begin{aligned} \phi_0(m+1) &= \phi_0(m) - P_0(m)\Delta\Phi, \\ &\cdots \\ \phi_{j+1}(m+1) &= \phi_{j+1}(m) + P_j(m)\Delta\Phi - P_{j+1}(m)\Delta\Phi, \\ &\cdots \\ \phi_N(m+1) &= \phi_N(m) + P_{N-1}(m)\Delta\Phi. \end{aligned} \tag{3}$$

It is notable that for large values of Φ the system does not necessarily reach equilibrium or a steady state. This is possible, however, at some specific p_i values when, for example, they depend on the configuration and tend to zero as $\Phi \to \infty$. In the current work we focus on nonequilibrium distributions and do not address such cases.

In the thermodynamic limit, the numbers of sites and particles are very large, and m is directly connected to the achieved site occupation $\Phi = m/K$. From this it follows that system (3) can be rewritten as

$$d\phi_0(\Phi) = -P_0(\Phi)d\Phi \tag{4a}$$

$$\cdots$$

$$d\phi_{j+1}(\Phi) = [P_j(\Phi) - P_{j+1}(\Phi)]d\Phi \tag{4b}$$

$$\cdots$$

$$d\phi_N(\Phi) = P_{N-1}(\Phi)d\Phi. \tag{4c}$$

Substitution of P_n from Eq. (1) into system (4) gives

$$\begin{aligned} d\phi_0 &= -Q\phi_0 p_0 d\Phi \\ &\cdots \\ d\phi_{j+1} &= Q(\phi_j p_j - \phi_{j+1} p_{j+1})d\Phi \\ &\cdots \\ d\phi_N &= Q\phi_{N-1} p_{N-1} d\Phi. \end{aligned} \tag{5}$$

The corresponding differential equations are

$$\frac{d\phi_1}{d\phi_0} = s_1\frac{\phi_1}{\phi_0} - 1, \tag{6a}$$

$$\frac{d\phi_2}{d\phi_0} = \frac{s_2\phi_2 - s_1\phi_1}{\phi_0}, \qquad \cdots \tag{6b}$$

where $s_n \equiv p_n/p_0$. With the initial conditions $\phi_0 = 1$, $\phi_1 = \phi_2 = \cdots = 0$ at $m = 0$ these equations allow one to obtain the partial occupied quantities ϕ_n for $n > 0$ for a given ϕ_0. Thus, when the relative probabilities p_i/p_0 remain constant during the assembly process, Eq. (6a) has the following solution:

$$\phi_1 = \left(\phi_0^{s_1} - \phi_0\right)/(1 - s_1). \tag{7}$$

Substitution into Eq. (6b) under the same conditions has the solution

$$\phi_2 = \frac{s_1}{(1-s_1)(1-s_2)}\left(\phi_0 - \frac{1-s_2}{s_1-s_2}\phi_0^{s_1} + \frac{1-s_1}{s_1-s_2}\phi_0^{s_2}\right). \tag{8}$$

In the "hard sphere" regime, when $p_1 = 0$, particles cannot occupy the same site, so that the fractions of the total number of sites covered by one and two particles reduce to $\phi_1 = 1 - \phi_0$ and $\phi_2 = 0$, respectively.

The general solution of system (6) is of the form

$$\phi_n = \sum_{k=1}^{n} a_k^{(n)}\phi_0^{s_k} + b^{(n)}\phi_0, \tag{9}$$

where the coefficients $a_k^{(n)}$ and $b^{(n)}$ are obtained after substituting Eq. (9) into Eqs. (6):

$$\begin{aligned} a_k^{(n)} &= \frac{1}{s_n}\frac{s_k}{1-s_k}\prod_{i=1,i\neq k}^{n}\frac{s_i}{s_i - s_k}, \\ b^{(n)} &= \frac{1}{s_n}\prod_{i=1}^{n}\frac{-s_i}{1-s_i}. \end{aligned} \tag{10}$$

For the highest occupancy term ϕ_N, the coefficients $a_k^{(N)}$ and $b^{(N)}$ must be evaluated in the limit $p_N = 0$ as it is not possible for the $(N+1)$th particle to bind to the site with highest occupancy. Note that ϕ_N can also be found after calculating the occupancies of lower orders as $\phi_N = 1 - \phi_0 - \phi_1 - \cdots - \phi_{N-1}$.

If there is no preferential binding, each p_i is the same constant for all i and can be set arbitrarily to 1 as only the ratios p_i/p_j play a role. In this case, $Q = 1$ and the solution for the occupied SF of the first equation in system (5) is $\phi = 1 - \phi_0 = 1 - \exp(-\Phi)$. It corresponds exactly to the Poisson limit [38,39] wherein Eqs. (7) and (8) reduce to

$$\begin{aligned} \phi_1 &\xrightarrow{p_1 \to p_0} -\phi_0 \ln\phi_0 = \Phi\exp(-\Phi), \\ \phi_2 &\xrightarrow[p_2 \to p_0]{p_1 \to p_0} \frac{\phi_0}{2}\ln^2\phi_0 = \frac{\Phi^2}{2}\exp(-\Phi). \end{aligned} \tag{11}$$

This Poisson distribution is also recovered for all terms, $\phi_n = \Phi^n\exp(-\Phi)/n!$, directly from system (5) as $s_i \to 1\ \forall\, i$. This is a known solution for clustering by irreversible filling [40,41] at equal filling rates. Another limiting case occurs when each site can accept only one particle (that is, $p_0 = 1$ and $p_i = 0$ for $i > 0$). Therein the solution of system (4) is $\phi_0 = 1 - \Phi$ and $\phi_1 = \Phi$.

Although system (5) cannot be solved easily for arbitrary values of $\{p_i\}$, analytic solutions are available in several nontrivial cases. For example, if high-order occupancies appear with small probabilities, one can neglect partial SFs with order larger than, say, m and assume that $\phi_0 + \phi_1 + \cdots + \phi_m \approx 1$. The smallest nontrivial set corresponds to $m = 1$, wherein $\phi_0 + \phi_1 \approx 1$. Combining Eq. (4a) with Eqs. (1) and (2) gives

$$d\Phi = -d\phi_0\,[\phi_0 + s_1(1-\phi_0)]/\phi_0, \tag{12}$$

which is solved to yield

$$\Phi = (1-s_1)(1-\phi_0) - s_1\ln\phi_0. \tag{13}$$

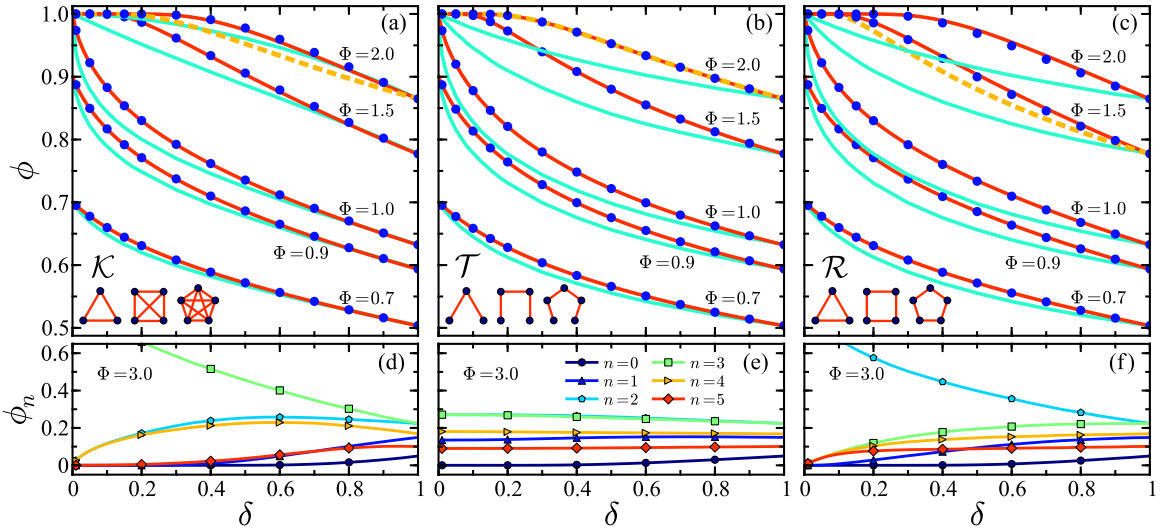

FIG. 1. (Color online) The probability of site occupation ϕ as a function of δ at various density values Φ for three interaction networks: (a) complete $\mathcal{K}$, (b) tethered $\mathcal{T}$, and (c) ring $\mathcal{R}$. The blue circular markers, orange dashed curves, and red solid curves correspond to the simulation, the first-order approximation in Eq. (14), and the second-order approximation in Eq. (16), respectively. The lower cyan solid curves in the top panels correspond to the equilibrium values of ϕ as measured from simulation. The insets in each panel are graphs of corresponding networks for $n = \{3,4,5\}$ particles. (d)–(f) The probability ϕ_n for observing n particles in a site as a function of δ for the corresponding network (shown above), as measured from simulation.

It then follows that

$$\phi = 1 - \frac{s_1}{1-s_1} W\left[\frac{1-s_1}{s_1}\exp\left(\frac{1-s_1-\Phi}{s_1}\right)\right], \qquad (14)$$

where W is the product logarithm [42]. For the second-order approximation ($m = 2$, $\phi_0 + \phi_1 + \phi_2 \approx 1$), Eq. (4a) reads

$$d\Phi = -d\phi_0 \, \frac{\phi_0 + s_1\phi_1 + s_2(1-\phi_0-\phi_1)}{\phi_0}, \qquad (15)$$

where ϕ_1 is taken from Eq. (7). The solution to this equation is

$$\Phi = \left(1 + s_1\frac{s_2-1}{1-s_1}\right)(1-\phi_0) + \frac{s_1-s_2}{s_1(1-s_1)}\left(1-\phi_0^{s_1}\right) - s_2\ln\phi_0. \qquad (16)$$

Equations (13) and (16) are valid for any arrival-initiated assembly process evolving through system (3) and constitute a central analytical result of this work. They relate the probability of site occupation $\phi = 1-\phi_0$ to density Φ, site occupation numbers ϕ_n [via Eqs. (7)–(9)], and site binding probabilities $\{p_n\}$. Higher-order approximations for ϕ can be obtained by solving differential equations like the ones above for a given m, although for brevity we refrain from producing these expressions here. Below, we show that the first- and second- order approximations adequately describe site occupation and structural growth at densities large enough to observe assembly behavior.

Thus far we have placed no constraints on the energetics with respect to arriving-particle–site and arriving-particle–bound-particle interactions. The makeup of these energies is represented through the probability ratios s_i. We consider here three energetic interaction networks: complete $\mathcal{K}$, tethered $\mathcal{T}$, and ring $\mathcal{R}$. For simplicity, we ignore particle-site interactions in all three cases; that is, we set $p_0 = 1$. In the complete interaction network $\mathcal{K}$, incident particles interact with every particle already bound to that site. Taking the energy between particles to be ϵ, the energy levels of $\mathcal{K}$ are $\{E_1 = 0, E_2 = \epsilon, E_3 = 3\epsilon, E_4 = 6\epsilon, \ldots, E_k = \epsilon k(k-1)/2\}$. Multiple occupancy lattice structures, cluster crystals, and aggregation of soft matter [19,43,44] are systems that have complete interaction networks. In the tethered network, an arriving particle interacts only with the site's top layer generating energy levels $\{E_1 = 0, E_2 = \epsilon, E_3 = 2\epsilon, \ldots, E_k = (k-1)\epsilon\}$. Polymerization and surface-initiated assembly of linear motifs are paradigmatic examples of tethered energetics [45–48]. In the ring network, the energy levels are $\{E_1 = 0, E_2 = \epsilon, E_3 = 3\epsilon, E_4 = 4\epsilon, \ldots, E_k = k\epsilon : k > 2\}$, corresponding to the assembly of systems such as ring polymers [49,50]. Representative graphs showing single-site interaction networks for the $\mathcal{K}$, $\mathcal{T}$, and $\mathcal{R}$ cases are shown in the bottom left corner of Figs. 1(a), 1(b), and 1(c), respectively. Other complex connectivity graphs can arise from alternative symmetries within the generated clusters [51,52] but can be accounted for through analogous considerations in the ϕ_n terms through the p_n parameters.

The acceptance probabilities $\{p_n\}$ for the three selected connectivity networks are a function of the parameter $\delta = \exp(-\epsilon^\star)$, where $\epsilon^\star = \epsilon/k_B T$ is the strength of the interaction. Specifically, $p_n = \delta^n$ in the complete case $\mathcal{K}$, $p_n = \delta$ for $\mathcal{T}$, and $\{p_1 = \delta, p_2 = \delta^2, p_n = \delta : n > 2\}$ for system $\mathcal{R}$. The limiting values of δ correspond to completely repulsive incident interactions or low temperature ($\delta = 0$) and soft incident interactions or high temperature ($\delta = 1$).

III. NUMERICAL RESULTS AND DISCUSSION

As shown in Fig. 1, Eq. (16) is in excellent agreement with the results obtained by sampling the sequentially generated structures through Monte Carlo (MC) simulations across

all ranges of density and interaction strengths and for all interaction networks. Note that in the tethered case the first- and second-order approximations are equivalent as $s_1 = s_2 = \delta$. At each step of the sequentially generated case, for example, a site is first chosen at random. An incident particle binds to it according to the acceptance probability $\{p_n\}$, which depends on the parameter δ. Note that the specific nature of these probabilities will depend on the chosen energetic connectivity network. If the particle is rejected by the chosen site, a new site is selected (with all sites equally likely), and the acceptance-rejection loop is repeated. If the particle is accepted by the site, the acceptance-rejection algorithm is initiated for the next particle in sequence. Further details about the simulations may be found in Ref. [33].

The canonical equilibrium site occupation probability can be obtained through a sum over the Boltzmann-weighted probabilities for each energetic state [33]. To measure this probability, Metropolis MC sampling [53] was performed on each interaction network over varying values of Φ and δ. In these simulations, after an initial relaxation phase, state sampling was initiated, and the Boltzmann-weighted ensemble average of these spatial states is the measured numerical result for ϕ. As shown in Fig. 1, values of ϕ generated by the equilibrium ensemble deviate significantly (and are less than) from those generated through a sequential arrival procedure. This observed lowering in the site occupation probability results from the clustered states that are formed through sequential assembly when a system is allowed to relax to an equilibrium state. This behavior is conjectured to persist across all energetic interaction networks, as the relaxation to equilibrium inherently relaxes the energetics encountered in the arrival process. The overall change in the energetics is not entirely determined by the clustering energy E, which may be positive or negative depending on the sign of ϵ, as it must also include the (unrelaxed) entropy term S. Thus, although in our case E increases, the free energy $E - TS$ can decrease through the equilibrium relaxation.

The generated nonequilibrium distributions are highly dependent on the interaction network and the pairwise interaction strength δ (see Fig. 1). For all three selected connectivity networks, the values of ϕ_n are in agreement in the Poisson distributed ($\delta = 1$) limit, as every particle is completely decorrelated. In the complete case $\mathcal{K}$, for small δ values, the distribution is dominated by a single high-order ϕ_n ($n = 3$), showing that aggregate size is strongly uniform. For tethered interactions, across all values of δ, approximately constant behavior is observed, and thus, the assembly distribution is Poisson-like. This result is in agreement with behavior observed in the assembly of polymer-grafted nanoparticles [48]. For systems $\mathcal{R}$, the dimers prevail at small δ, showing that formation of ring structures is more energetically consuming, whereas at $\delta > 0.8$ the overall structure resembles that of the tethered case $\mathcal{T}$.

Figure 2 shows the growth of ϕ with respect to variation in Φ. In the Poisson limit, a characteristic exponential (linear behavior in the semilog inset) is observed in accordance with Eq. (11). A distinct turnover (sigmoidal behavior) in the occupancy gradient is observed below the Poisson distributed

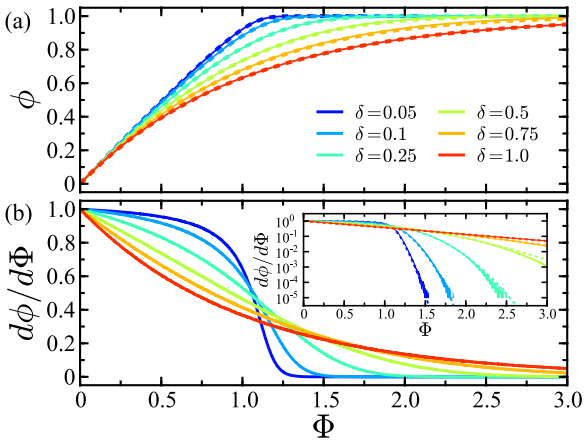

FIG. 2. (Color online) (a) The probability of site occupation ϕ and (b) growth $d\phi/d\Phi$ as a function of density Φ for various values of δ. The energetics correspond to the complete interaction case $\mathcal{K}$. The inset shows the growth rate on a log scale. The solid curves are the results measured from simulation, and the dashed curves are the results given by Eq. (16).

limit. At small δ values, initially sparse organization is observed due to multiple rejections from occupied sites. After the turnover point, where the derivative $d\phi/d\Phi$ at $\delta < 1$ crosses that at $\delta = 1$, layers are formed, and the binding preference of an incident particle shifts from unoccupied to occupied sites. This is correlated with the approach of the occupation probability toward the asymptotic value $\phi = 1$, which corresponds to complete covered binding sites. It is interesting to note that at large values of Φ the derivative $d\phi/d\Phi$ approaches exponential behavior. The latter can be directly obtained from Eq. (16) evaluated at small ϕ_0 (a large density of adsorbed particles leads to a small number of vacancies):

$$\frac{d\phi}{d\Phi} = -\frac{d\phi_0}{d\Phi} \sim \exp(-\Phi/s_2)\ . \tag{17}$$

IV. CONCLUSIONS

In summary, we have developed a theoretical formulation for the structures generated through an arrival process in which monomeric objects sequentially assemble. We find that the distribution in the size of tethered linear aggregates with varying interaction strength is approximately Poissonian, whereas it takes more complex forms for other connectivity networks. Such characterization allows for the design of novel materials quenched from intrinsically nonequilibrium distributions of site occupation through the control of the interaction network and strength.

Note added. We have recently become aware of a concurrently published study by Osberg *et al.* [54] in which a one-dimensional model was introduced to consider the absorption and desorption kinetics of soft particles. Like us, they found significant effects due to the introduction of soft-particle interactions. The model presented here also includes the possibility of surface adsorption (in two dimensions) and more general dimensionality depending on the topology

of the connectivity network. Observation of the phenomena predicted in these studies would provide impetus for additional theoretical and experimental inquiry into the role that softness plays in adsorption.

ACKNOWLEDGMENTS

This work has been partially supported by the National Science Foundation (NSF) through Grant No. NSF-CHE-1112067.

[1] S. C. Glotzer, Science **306**, 419 (2004).
[2] Q. Wang, Soft Matter **5**, 4564 (2009).
[3] Q. Wang, Soft Matter **7**, 3711 (2011).
[4] N. Marshall, S. K. Sontag, and J. Locklin, Chem. Commun. (Cambridge, UK) **47**, 5681 (2011).
[5] N. Duff and B. Peters, J. Chem. Phys. **131**, 184101 (2009).
[6] R. J. Davey, S. L. M. Schroeder, and J. H. ter Horst, Angew. Chem., Int. Ed. **52**, 2166 (2013).
[7] G. G. Poon and B. Peters, Cryst. Growth Des. **13**, 4642 (2013).
[8] S. A. Sanders and A. Z. Panagiotopoulos, J. Chem. Phys. **132**, 114902 (2010).
[9] C. Georgiadis, O. Moultos, L. N. Gergidis, and C. Vlahos, Langmuir **27**, 835 (2011).
[10] Y. Ke, L. L. Ong, W. M. Shih, and P. Yin, Science **338**, 1177 (2012).
[11] A. Reinhardt and D. Frenkel, Phys. Rev. Lett. **112**, 238103 (2014).
[12] C. N. Likos, Phys. Rep. **348**, 267 (2001).
[13] C. N. Likos, S. Rosenfeldt, N. Dingenouts, M. Ballauff, P. Lindner, N. Werner, and F. Vogtle, J. Chem. Phys. **117**, 1869 (2002).
[14] M. Ballauff and C. N. Likos, Angew. Chem., Int. Ed. **43**, 2998 (2004).
[15] T. Dotera, T. Oshiro, and P. Ziherl, Nature (London) **506**, 208 (2014).
[16] K. Barkan, M. Engel, and R. Lifshitz, Phys. Rev. Lett. **113**, 098304 (2014).
[17] A. J. Archer, A. M. Rucklidge, and E. Knobloch, Phys. Rev. Lett. **111**, 165501 (2013).
[18] B. M. Mladek, G. Kahl, and M. Neumann, J. Chem. Phys. **124**, 064503 (2006).
[19] B. M. Mladek, D. Gottwald, G. Kahl, M. Neumann, and C. N. Likos, Phys. Rev. Lett. **96**, 045701 (2006).
[20] B. M. Mladek, P. Charbonneau, C. N. Likos, D. Frenkel, and G. Kahl, J. Phys. Condens. Matter **20**, 494245 (2008).
[21] K. Zhang and P. Charbonneau, J. Chem. Phys. **136**, 214106 (2012).
[22] D. Coslovich and A. Ikeda, Soft Matter **9**, 6786 (2013).
[23] G. T. Craven, A. V. Popov, and R. Hernandez, J. Chem. Phys. **138**, 244901 (2013).
[24] G. T. Craven, A. V. Popov, and R. Hernandez, Soft Matter **10**, 5350 (2014).
[25] G. T. Craven, A. V. Popov, and R. Hernandez, J. Chem. Phys. **142**, 154906 (2015).
[26] J. T. Kindt, J. Chem. Theory Comput. **9**, 147 (2013).
[27] B. M. Rankin and D. Ben-Amotz, J. Phys. Chem. B **117**, 15667 (2013).
[28] D. Ben-Amotz, B. M. Rankin, and B. Widom, J. Phys. Chem. B **118**, 7878 (2014).
[29] M. Möddel, W. Janke, and M. Bachmann, Phys. Rev. Lett. **112**, 148303 (2014).
[30] C. Jarzynski, Nat. Phys. **11**, 105 (2015).
[31] B. Widom, J. Chem. Phys. **44**, 3888 (1966).
[32] S. Torquato, O. U. Uche, and F. H. Stillinger, Phys. Rev. E **74**, 061308 (2006).
[33] G. T. Craven, A. V. Popov, and R. Hernandez, J. Phys. Chem. B **118**, 14092 (2014).
[34] J. Feder, J. Theor. Biol. **87**, 237 (1980).
[35] M. Cieśla, J. Stat. Mech. (2013) P07011.
[36] M. Cieśla and P. Karbowniczek, Phys. Rev. E **91**, 042404 (2015).
[37] S. L. James, Chem. Soc. Rev. **32**, 276 (2003).
[38] S. Torquato, B. Lu, and J. Rubinstein, Phys. Rev. A **41**, 2059 (1990).
[39] J. Quintanilla and S. Torquato, Phys. Rev. E **54**, 5331 (1996).
[40] J. W. Evans, J. A. Bartz, and D. E. Sanders, Phys. Rev. A **34**, 1434 (1986).
[41] P. I. Cohen, G. S. Petrich, P. R. Pukite, and G. J. Whaley, Surf. Sci. **216**, 222 (1989).
[42] R. M. Corless, G. H. Gonnet, D. E. G. Hare, D. J. Jeffrey, and D. E. Knuth, Adv. Comput. Math. **5**, 329 (1996).
[43] R. Finken, J.-P. Hansen, and A. A. Louis, J. Phys. A **37**, 577 (2004).
[44] C. N. Likos, Soft Matter **2**, 478 (2006).
[45] A. Santos, C. Singh, and S. C. Glotzer, Phys. Rev. E **81**, 011113 (2010).
[46] C. L. Phillips and S. C. Glotzer, J. Chem. Phys. **137**, 104901 (2012).
[47] M. R. Farrow, P. J. Camp, P. J. Dowding, and K. Lewtas, Phys. Chem. Chem. Phys. **15**, 11653 (2013).
[48] M. Asai, A. Cacciuto, and S. K. Kumar, Soft Matter **11**, 793 (2015).
[49] A. Narros, A. J. Moreno, and C. N. Likos, Soft Matter **6**, 2435 (2010).
[50] L. J. Abbott and C. M. Colina, J. Chem. Eng. Data **59**, 3177 (2014).
[51] G. Meng, N. Arkus, M. P. Brenner, and V. N. Manoharan, Science **327**, 560 (2010).
[52] J. Guzowski and P. Garstecki, Phys. Rev. Lett. **114**, 188302 (2015).
[53] N. Metropolis, A. W. Rosenbluth, M. N. Rosenbluth, A. H. Teller, and E. Teller, J. Chem. Phys. **21**, 1087 (1953).
[54] B. Osberg, J. Nuebler, and U. Gerland, Phys. Rev. Lett. **115**, 088301 (2015).